

Supporting Information for:

Low temperature glass/crystal transition in ionic liquids determined by H-bond vs. Coulombic strength

C. López-Bueno^a, M. Bittermann^b, B. Dacuña-Mariño^c, A. L. Llamas-Saiz^c, M. C. Giménez-López^{a,d}, S. Woutersen^b, and F. Rivadulla^{*,a,e}

^aCIQUS, Centro de Investigación en Química Biolóxica e Materiais Moleculares, Universidade de Santiago de Compostela, 15782-Santiago de Compostela, Spain. Email: f.rivadulla@usc.es

^bVan't Hoff Institute for Molecular Sciences, University of Amsterdam, Science Park 904, 1098 XH Amsterdam, Netherlands.

^cX-Ray Unit, RIAIDT, Universidade de Santiago de Compostela, 15782 Santiago de Compostela, Spain.

^dDepartamento de Química-Inorgánica, Universidade de Santiago de Compostela, 15782-Santiago de Compostela, Spain.

^eDepartamento de Química-Física, Universidade de Santiago de Compostela, 15782-Santiago de Compostela, Spain.

Table S1: Different transition temperatures observed for the ionic liquids studied in this work. T_c , and T_m , refer to the temperature of formation and melting of a crystal or a liquid crystal phase, respectively, as observed in the thermal conductivity and DSC data. For liquids (4) to (8) the crystals nucleate within a glassy phase, as obtained also from POM experiments and explained in the text. T_g , refers to the formation of the glass, also obtained from thermal conductivity and DSC. The numbers in the first column identify the different ionic liquids, as follows: **(1)** 1-Ethyl-2,3-dimethylimidazolium bis(trifluoromethylsulfonyl)imide; **(2)** 1-Ethyl-3-Methylimidazolium bis(trifluoromethylsulfonyl)imide; **(3)** 1-Butyl-3-Methylimidazolium triflate; **(4)** 1-Ethylimidazolium bis(trifluoromethylsulfonyl)imide; **(5)** 1-Butyl-3-Methylimidazolium nitrate; **(6)** 1-Ethyl-3-Methylimidazolium acetate.

	T_c / K	T_m / K	T_g / K
(1)	240	290	
(2)	225	250	
(3)	231	281	
(4)	137	186	197
(5)	150	190	212
(5)	100	180	200
(7)	155	195	215
(8)	139	180	195

EFFECT OF WATER: INITIAL DRYING OF THE LIQUIDS

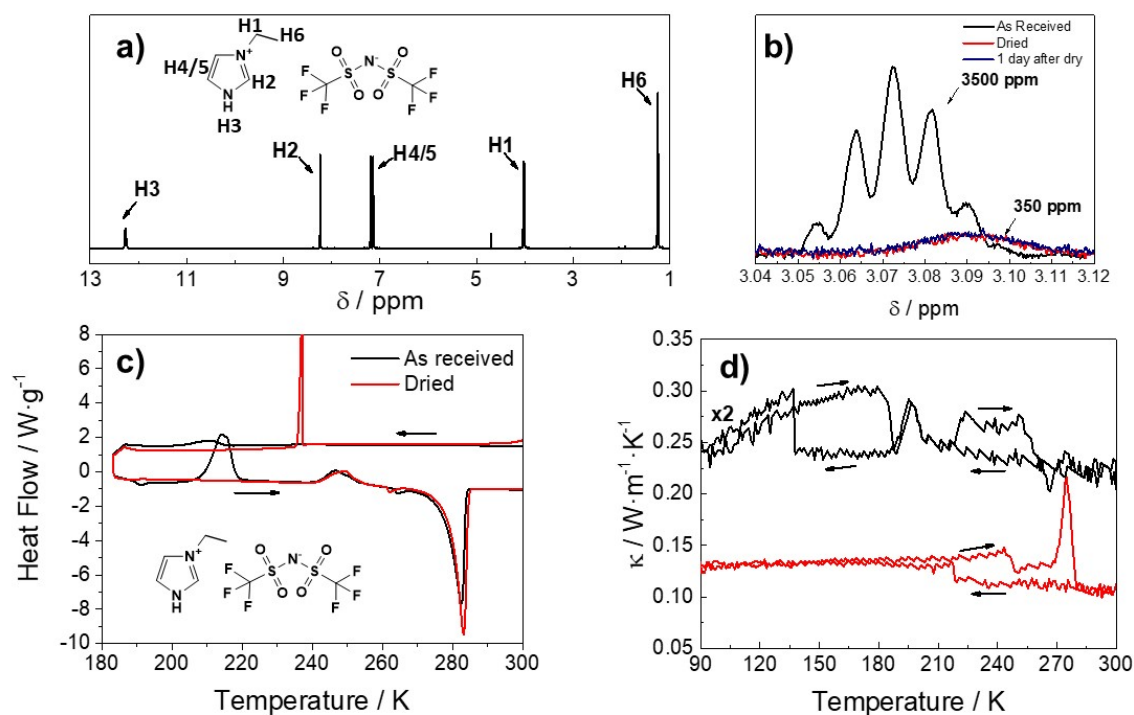


Figure S1. H-NMR of liquid (4) a) and detail of the region around 3.07 ppm b), showing the signal of water H-bonded to different protons of the cation. The water content decreases down to 350 ppm after drying and remains practically constant after 1 day in a glove box. The DSC and thermal conductivity measurements shown in c) and d) for the humid and dried phases show the strong suppression of the crystal phase by water.

EFFECT OF REDUCED MASS ON THE DISPLACEMENT OF THE FAR-IR PEAKS

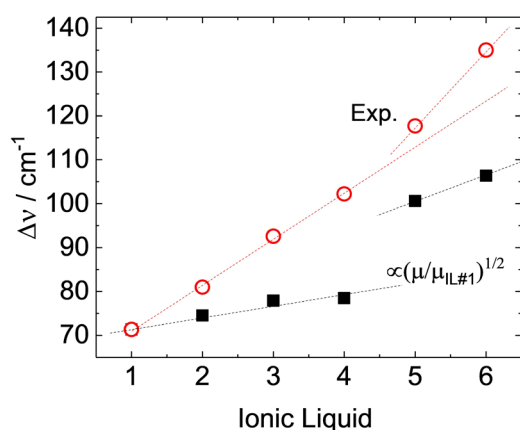


Figure S2. Experimental frequency shift of the far-IR band for the different ionic liquids studied in this work (open circles). Calculated frequency shift according to the change in the reduced mass of the ion pairs of the ionic liquids (solid squares). The effect of the reduced mass has been calculated from the harmonic oscillator approximation: $\nu \propto (\kappa/\mu)^{1/2}$. Lines are guides to the eye.

DIFFERENTIAL SCANNING CALORIMETRY

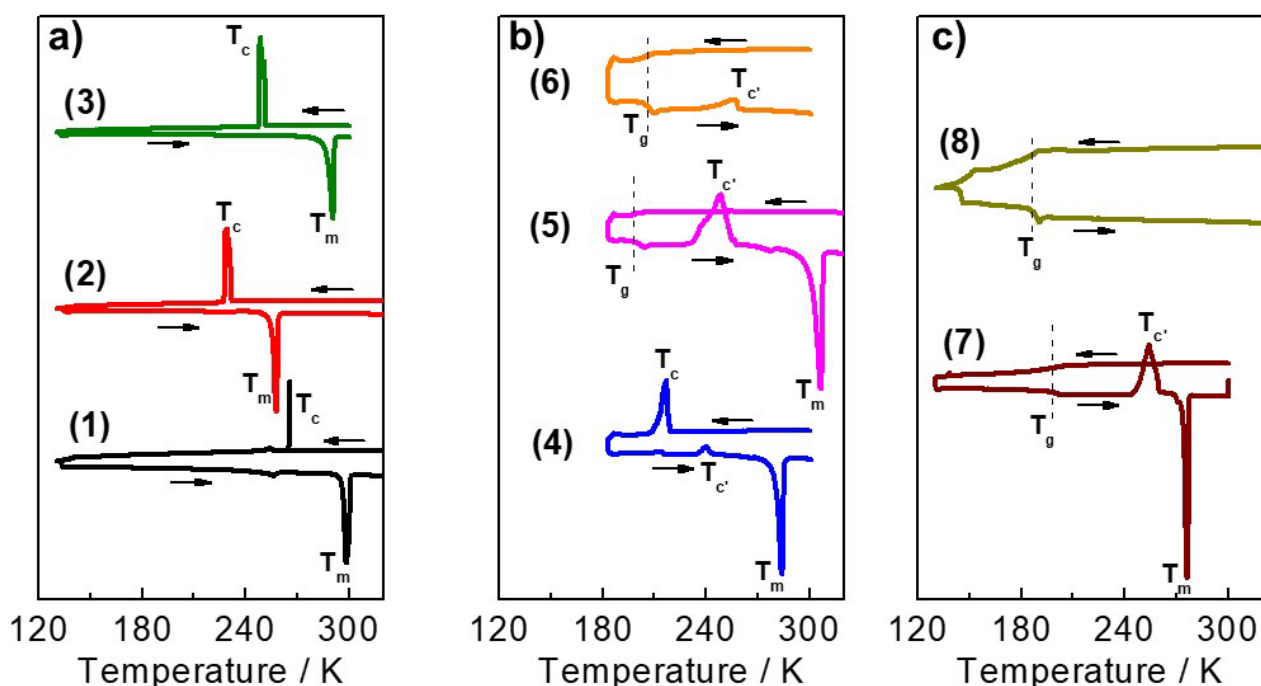


Figure S3. Differential scanning calorimetry (DSC) of the Im-ILs studied in this work. Temperature ramps are fixed to 2K/min for all curves. T_c , T_m , and T_c' correspond to the crystallization, melting and recrystallization temperatures, respectively. T_g refers to the glass transition temperature. The vertical dotted lines at T_g mark the drop characterizing the glass transition at the same temperature on cooling and warming ramps.

STUDY OF IMIDAZOLE IONIC LIQUIDS WITH LONG ALKYL CHAINS

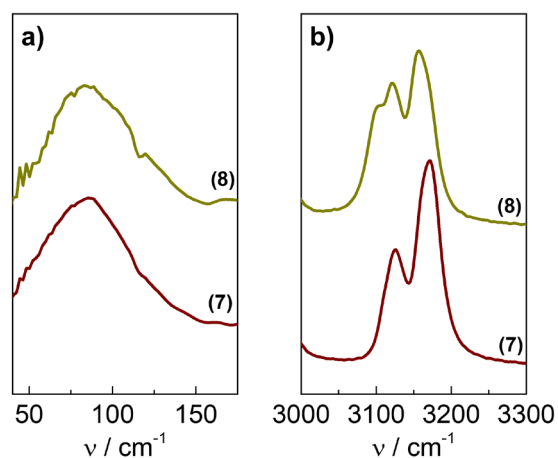


Figure S4. IR-spectra for two of the Im-ILs studied in this work. **(7)**: 1-Octyl-3-methylimidazolium hexafluorophosphate (MOIM-PF₆); **(8)** 1-Octyl-3-methylimidazolium bis(trifluoromethylsulfonyl)imide (MOIM-NTF₂).

ADDITIONAL X-RAY AND POM EXPERIMENTS

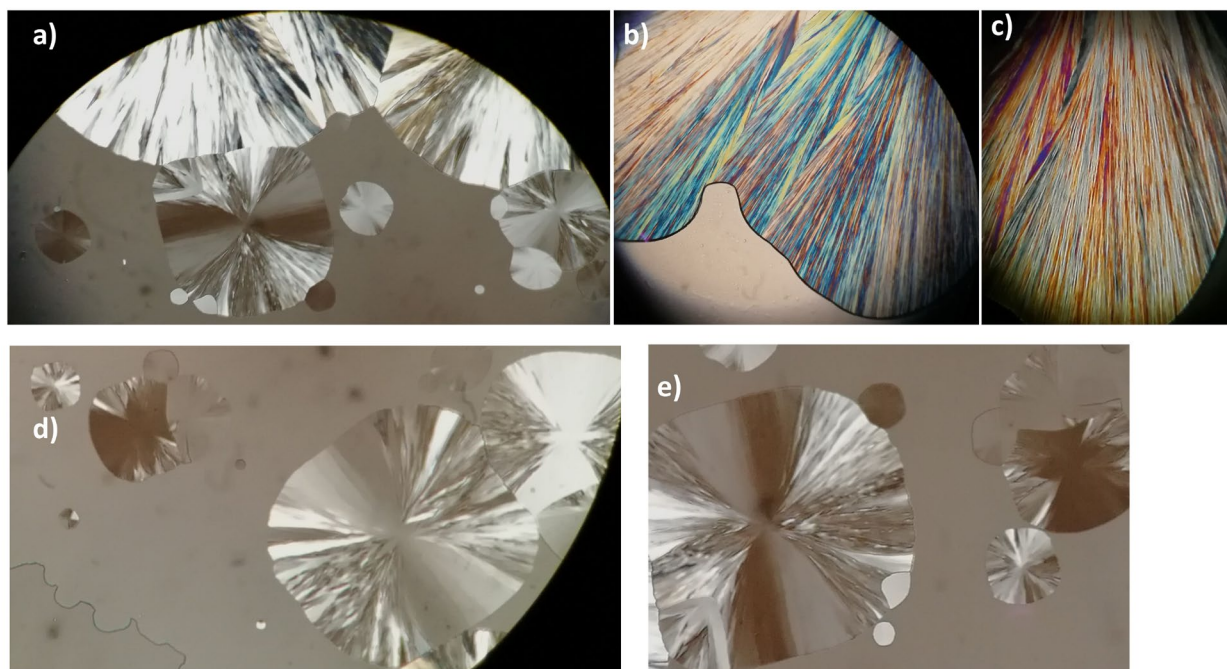


Figure S5. POM images of the semi-crystalline phases developed at low temperature in liquid **(3)**. Different colors are observed in b) and c) by rotating the optical polarizers.

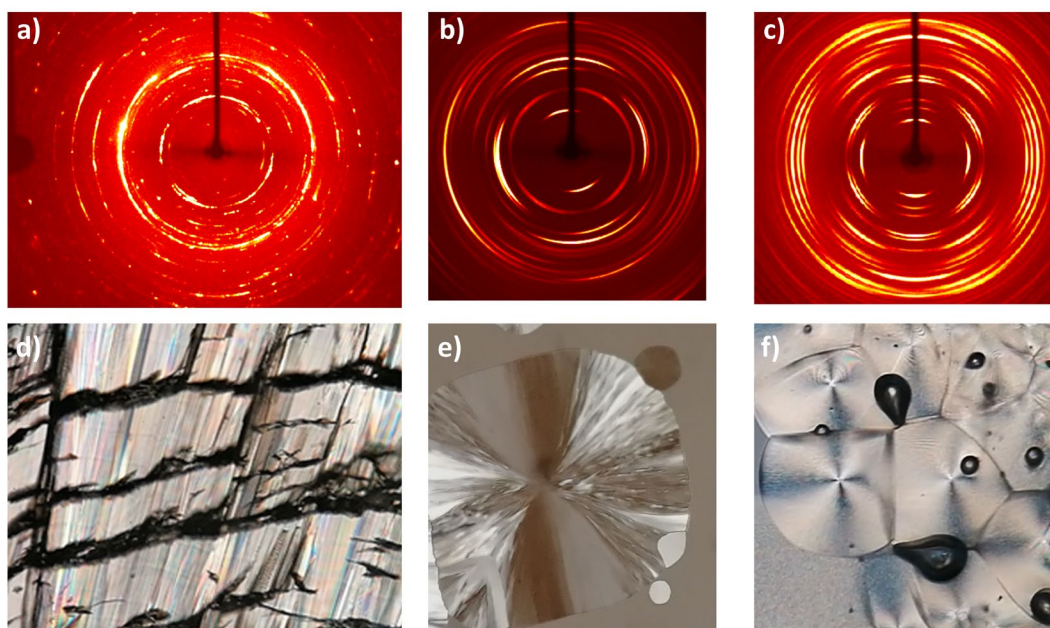


Figure S6. X-ray diffraction (top) and POM images (bottom) at low temperature of liquids **(1)** (X-ray shown in a) and POM picture in d), liquid **(3)** (X-ray shown in b) and POM image in e) and liquid **(5)** (X-ray shown in c) and POM image in f). The POM in d) show the typical crack lines of a crystalline system, consistent with the observation of single-crystal spots in the X-ray diffraction pattern shown in a). The POM image in e) and f) are consistent with columnar or nematic ordering. This is confirmed by the X-ray pattern shown in b) and c).

THERMODYNAMIC ANALYSIS OF THE LOW TEMPERATURE TRANSITION

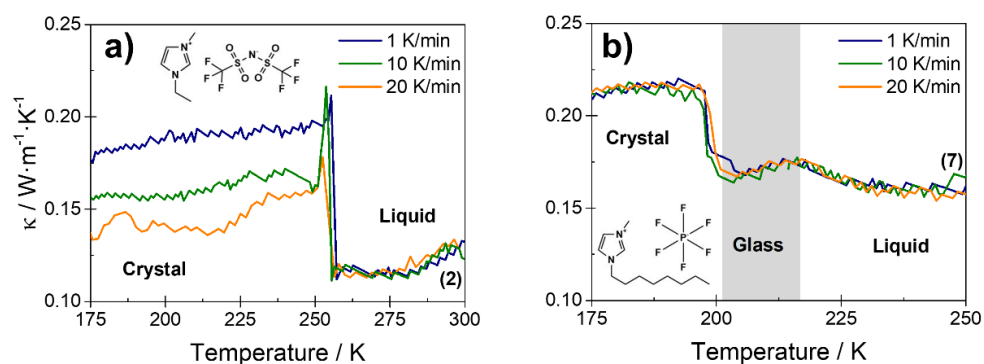


Figure S7. Temperature dependence of the thermal conductivity for a) EMIM-NTF₂ **(2)** and b) MOIM-PF₆ **(7)**. The measurements are performed during heating at 1K/min, but after cooling the samples at different rates (indicated).

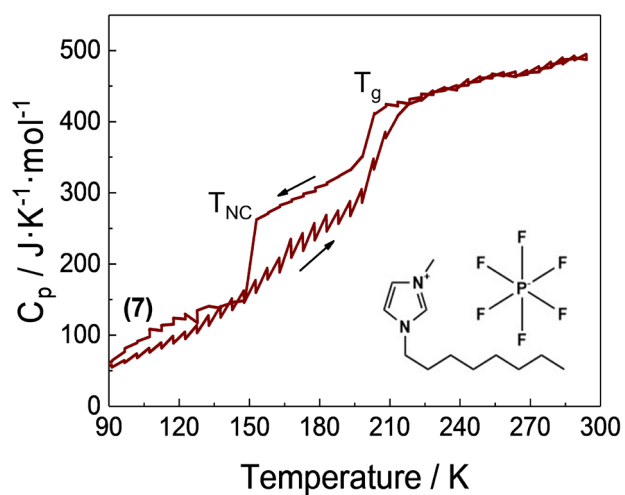


Figure S8. Temperature dependence of $C_p(T)$ for liquid **(7)**. There is a small increase of C_p at ≈ 270 K, the same temperature at which the thermal conductivity of the liquid flattens (see Figure 5c in the paper). C_p decreases sharply at T_g and T_{NC} and shows a thermal hysteresis which confirms the transitions observed in thermal conductivity measurements.

CRYO-IR MEASUREMENTS

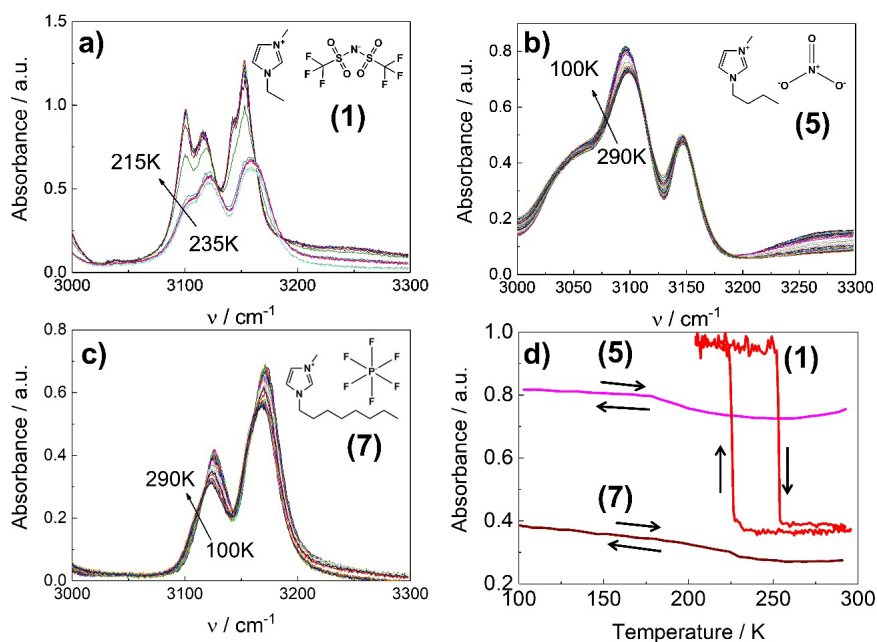


Figure S9. The reorganization of intermolecular bonds across T_{NC} was probed through temperature dependent IR absorption. a)- c) Temperature dependent FTIR spectra of liquids **(1)**, **(5)**, and **(7)** across the different transitions. Panel d) shows the absorbance at 3100 cm^{-1} for these liquids. Liquid **(1)** shows a sudden increase of the absorption at the crystallization temperature and the thermal hysteresis consistent with the X-ray data. For **(5)** and **(7)** only a small change of slope is observed at T_{g} without any further feature at T_{NC} . The results discard a large change in the dipole moment due to the formation of new intermolecular bonds at T_{NC} .

RECRYSTALLIZATION

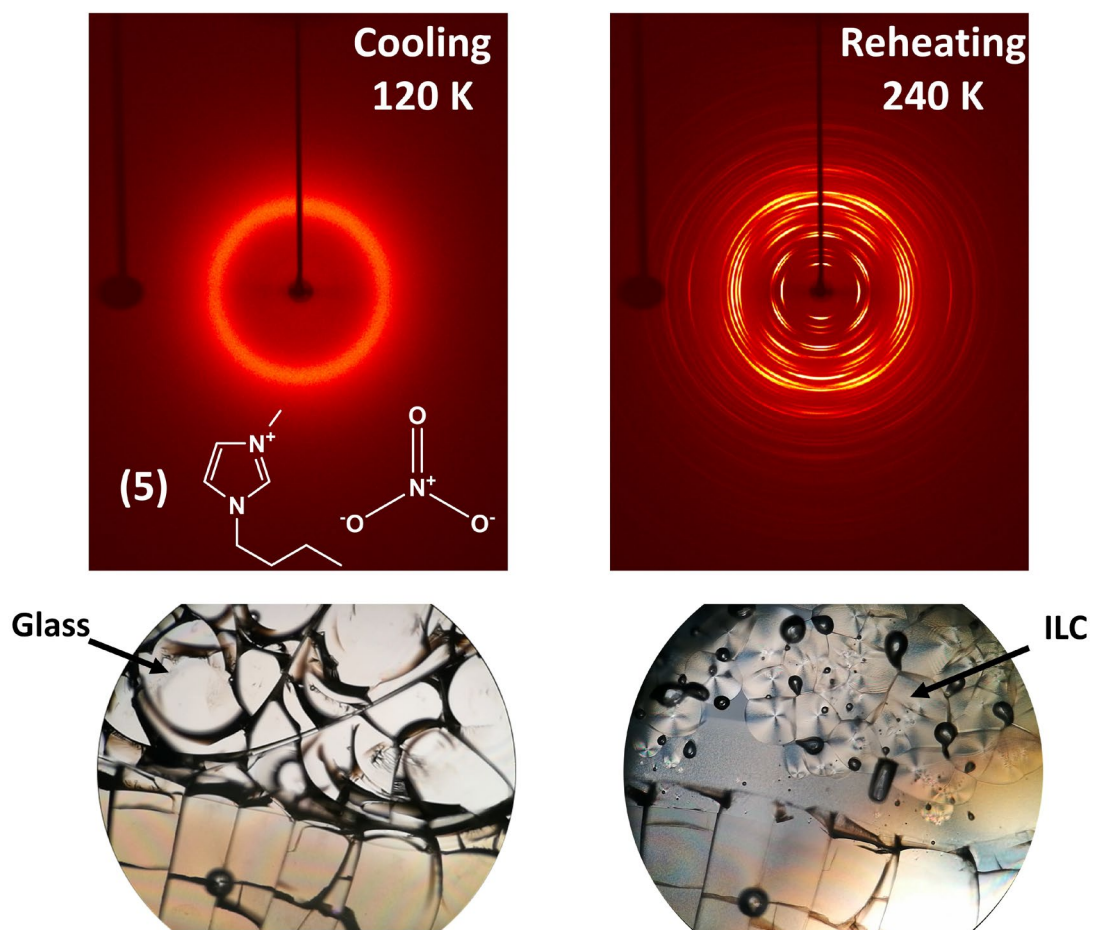


Figure S10. Formation of a glass on cooling liquid (5), and subsequent recrystallization on warming. The formation of the glass below T_g observed in POM images (bottom left) coincides with the sudden change of slope and thermal hysteresis of the thermal conductivity shown in Figure 4b). The temperature of recrystallization observed by X-ray diffraction (top) and POM images (bottom) match the T_c' observed by DSC in Figure S1. See also video 5b.